A Truncated Form of IKKα Is Responsible for Specific Nuclear IKK Activity in Colorectal Cancer

Pol Margalef,[1,8] Vanessa Fernández-Majada,[1,8,9] Alberto Villanueva,[3] Ricard Garcia-Carbonell,[1,2] Mar Iglesias,[2] Laura López,[2] María Martínez-Iniesta,[3] Jordi Villà-Freixa,[4] Mari Carmen Mulero,[1] Montserrat Andreu,[5] Ferran Torres,[6] Marty W. Mayo,[7] Anna Bigas,[1] and Lluis Espinosa[1,*]

[1]Institut Municipal d'Investigacions Mèdiques (IMIM)
[2]Department of Pathology
Institut Hospital del Mar d'Investigacions Mèdiques, Parc de Recerca Biomèdica de Barcelona, Barcelona 08003, Spain
[3]Laboratori de Recerca Translacional, IDIBELL-Institut Català d'Oncologia Gran Via km 2.7, Hospitalet, Barcelona 08907, Spain
[4]Computational Biochemistry and Biophysics Laboratory
[5]Department of Gastroenterology
IMIM-Hospital del Mar, Universitat Pompeu Fabra, Barcelona 08003, Spain
[6]Department of Statistics, UAB, Barcelona 08193, Spain
[7]Department of Biochemistry and Molecular Genetics, The University of Virginia, Charlottesville, VA 22908, USA
[8]These authors contributed equally to this work
[9]Present address: Institute for Genetics, University of Cologne, 50674 Cologne, Germany
*Correspondence: lespinosa@imim.es
http://dx.doi.org/10.1016/j.celrep.2012.08.028

SUMMARY

Nuclear IKKα regulates gene transcription by phosphorylating specific substrates and has been linked to cancer progression and metastasis. However, the mechanistic connection between tumorigenesis and IKKα activity remains poorly understood. We have now analyzed 288 human colorectal cancer samples and found a significant association between the presence of nuclear IKK and malignancy. Importantly, the nucleus of tumor cells contains an active IKKα isoform with a predicted molecular weight of 45 kDa (p45-IKKα) that includes the kinase domain but lacks several regulatory regions. Active nuclear p45-IKKα forms a complex with nonactive IKKα and NEMO that mediates phosphorylation of SMRT and histone H3. Proteolytic cleavage of FL-IKKα into p45-IKKα is required for preventing the apoptosis of CRC cells in vitro and sustaining tumor growth in vivo. Our findings identify a potentially druggable target for treating patients with advance refractory CRC.

INTRODUCTION

NF-κB is a transcription factor that regulates innate and acquired immune responses, inflammation, and cancer (Hayden and Ghosh, 2004; Hayden et al., 2006; Schulze-Luehrmann and Ghosh, 2006). In the absence of stimulation, NF-κB dimers (such as p65/p50) are primarily cytoplasmic and bound to the inhibitor of κB (IκB). Induction of canonical NF-κB pathway by specific stimuli, such as tumor necrosis factor (TNF)-α, bacterial and viral products, or DNA damage, leads to the activation of the IKK (IκB kinase) complex that phosphorylates IκB inducing its degradation and nuclear translocation of the NF-κB factor. The IKK complex is composed of two catalytic subunits, IKKα/IKK1 and IKKβ/IKK2, and the regulatory IKKγ/NEMO (for NF-κB Essential Modifier). Molecular weight of IKKα and IKKβ is 85 and 87 kDa, respectively, and they share 50% of amino acid identity and 70% of structural similarity. IKKα and β contain an amino-terminal kinase domain, a leucine zipper (LZ) region involved in protein dimerization and a helix-loop-helix (HLH) (DiDonato et al., 1997; Zandi et al., 1997). Recently, LZ and HLH regions of IKK have been redefined based on structural data of IKKβ (Xu et al., 2011). It is established that IKKβ and NEMO are essential mediators of IκB degradation and canonical NF-κB activation. Conversely, activation of IKKα by LTβ, CD40, or BAFF induces processing of p100 into p52. Then, p52/RelB dimers translocate to the nucleus and activate specific gene transcription. This signaling pathway, known as alternative NF-κB, is required for secondary lymphoid organogenesis (Senftleben et al., 2001).

In addition to its cytoplasmic functions, nuclear roles for IKKα have recently been identified such as binding to the chromatin of specific promoter regions to phosphorylate serine 10 of histone H3, which affects chromatin condensation and facilitates transcriptional activation of NF-κB-dependent and -independent genes (Anest et al., 2003, 2004; Park et al., 2005; Yamamoto et al., 2003). Nuclear IKKα also regulates cell-cycle progression through phosphorylation of the AuroraB kinase (Prajapati et al., 2006) and derepression of 14-3-3σ (Zhu et al., 2007b). In cancer cells, chromatin-bound IKKα activates the metastasis-related gene, maspin, through epigenetic modifications (Luo et al., 2007) and associates with other factors such as Notch to regulate specific transcription (Hao et al., 2010; Song et al., 2008; Vilimas et al., 2007). Moreover, IKKα activates

cIAP2 and IL-8 transcription through phosphorylation of the nuclear corepressor SMRT at serine 2410, which induces its cytoplasmic export and degradation (Hoberg et al., 2004). We previously demonstrated that colorectal cancer (CRC) cells contain nuclear IKKα, which phosphorylates SMRT and N-CoR leading to the activation of Notch-target genes hes1 and herp2 (Fernández-Majada et al., 2007a, 2007b). This is important since Notch activity is required for CRC progression (Fre et al., 2005; van Es et al., 2005). Interestingly, inhibition of IKK activity reverted Notch-target gene expression and reduced tumor xenografts growth in nude mice (Fernández-Majada et al., 2007a, 2007b). However, IKK activity is essential for multiple physiological functions, including regulation of immune response, differentiation of lymph nodes, mammary gland, and skin, and maintenance of liver and gut homeostasis (Luedde et al., 2007; Nenci et al., 2007; Pasparakis et al., 2002), and consequently, cannot be inhibited without producing severe undesirable effects (Chen et al., 2003; Greten et al., 2007; Maeda et al., 2005).

In this work, we study the traits that distinguish CRC-related IKK functions from those associated with physiological NF-κB, which has critical implications for further identification of therapeutic druggable targets. We show that nuclear localization of active IKKα is a common event associated with advanced human CRC, and identify a truncated form of IKKα (referred to as p45-IKKα) that represents the majority of active IKK in this cellular compartment. Truncated IKKα is generated by cathepsin activity, which is increased in CRC. At the biochemical level, active p45-IKKα is in a nuclear complex with NEMO, which specifically phosphorylates SMRT leading to specific gene transcription. Knocking down IKKα prevents growth of CRC cells both in vitro and in vivo, and this effect is rescued by small hairpin RNA (shRNA)-resistant IKKα but not by a cleavage-defective mutant. Together, our results indicate the possibility to target p45-IKKα generation or activation as a strategy for CRC treatment.

RESULTS

CRC Cells Contain a Nuclear Form of IKKα of 45 kDa
Activation of nuclear IKKα has been previously associated with human CRC and prostate metastasis in mouse (Fernández-Majada et al., 2007a; Luo et al., 2007). We here analyze a total of 288 samples (147 adenomas and 141 carcinomas) and the corresponding paired distal normal mucosa from 98 patients and found that more than 60% of the adenomas and 85% of the carcinomas show high P-IKK staining (considering ++ plus +++ intensities) compared with adjacent normal tissues (19% positive), as detected by immunohistochemistry (IHC) with two antibodies recognizing phosphorylated serines 180/181 of IKKα and β, respectively (α-P-IKK, Cell Signaling no. 2681 and Santa Cruz sc-23470) (Figures 1A and 1B). Most of the positive samples showed strong punctuate cytoplasmic staining; in addition 30% of adenomas and 40% of carcinomas contain detectable levels of nuclear P-IKK (Figures 1A, 1C, and 1D). Confocal microscopy confirmed the presence of nuclear P-IKK in 11 out of 12 randomly selected samples identified as nuclear positive in the general screening, and its absence in

12 out of 12 negative samples (96% correspondence). A more detailed analysis revealed that, even in the positive tumors, most of P-IKK was localized in cytoplasmic vesicles, being the nuclear staining restricted to discrete dots (Figure S1A; data not shown). To further investigate the nature of tumor-associated nuclear IKK, we performed subcellular fractionation followed by western blot analysis of fresh CRC samples and normal adjacent mucosa (N) from 4 different patients and 2 human carcinomas grown as xenograft in nude mice (CRCX). We found that most of the active P-IKK corresponding to the expected size of 85–87 kDa was localized in the cytoplasm of tumor and normal cells. Unexpectedly, the same antibody recognized a double band of around 45 kDa that was highly enriched in both the cytoplasmic and nuclear fractions of carcinoma cells (from now on p45-IKK) (Figure 1E). Active p45-IKK was also detected in human CRC cell lines using two different α-P-IKK antibodies (Cell Signaling no. 2681 and no. 2697) (Figure 1F) and from extracts obtained in the presence of specific protease inhibitors (Figure S1B, lanes 2 and 3) or directly boiled in 1% SDS sample buffer and electrophoresed without further manipulation (Figure S1B, lane 4). α-IKKα antibody, but not α-IKKβ, recognized bands compatible with p45-IKK in all tested CRC cells (Figure 1F) and human CRC samples (Figure 1E), suggesting that p45-IKK was an isoform of IKKα. Of note, that nonphosphorylated p45-IKK was also detected in the cytoplasm of nontransformed cells (Figure 1E). To further demonstrate that p45-IKK was a product of IKKα, we performed knockdown experiments in HCT116 and Ls174T cells, followed by western blot analysis. We found that different shRNA targeting IKKα reduced both the 85 kDa and the 45 kDa bands detected with α-IKKα antibody from total (Figure 1G) and nuclear extracts (Figure S1C). In contrast, IKKβ levels were not affected, demonstrating the specificity of the shRNA, although we observed a reduction of NEMO levels (Figures 1G and S1D) that did not affect canonical NF-κB activity as detected by IκBα phosphorylation after TNF-α treatment (Figure S1D). Besides, we detected low levels of p45-IKKα in mouse embryonic fibroblasts (MEFs) that were absent from IKKα knockout (KO) MEFs (Figure S1E) supporting the IKKα nature of p45. Importantly, antibodies recognizing phosphorylated IKK failed to detect this band (data not shown), as in normal human samples (Figure 1D), suggesting that p45-IKKα is inactive in nontransformed cells. Further demonstrating that p45-IKKα is phosphorylated in CRC, treatment of HCT116 nuclear extracts with calf intestinal alkaline phosphatase (CIAP) abrogated detection of p45-IKK by α-P-IKK (Figure S1F). These results indicate the existence of an IKKα species with an apparent size of 45 kDa that represents the majority of active IKK in the nucleus of CRC cells. Conversely, nontransformed cells contain nonphosphorylated p45-IKKα, which is localized in the cytoplasm.

Generation of the Nuclear p45-IKKα Form Present in CRC Cells
We tested the possibility that high levels of p45-IKKα found in CRC cells were due to mutations in the IKKα sequence that translate into a truncated protein. Because of its inferred molecular size, we focused on studying the region involving exons 13–15 of IKKα, which was found to be mutated in squamous
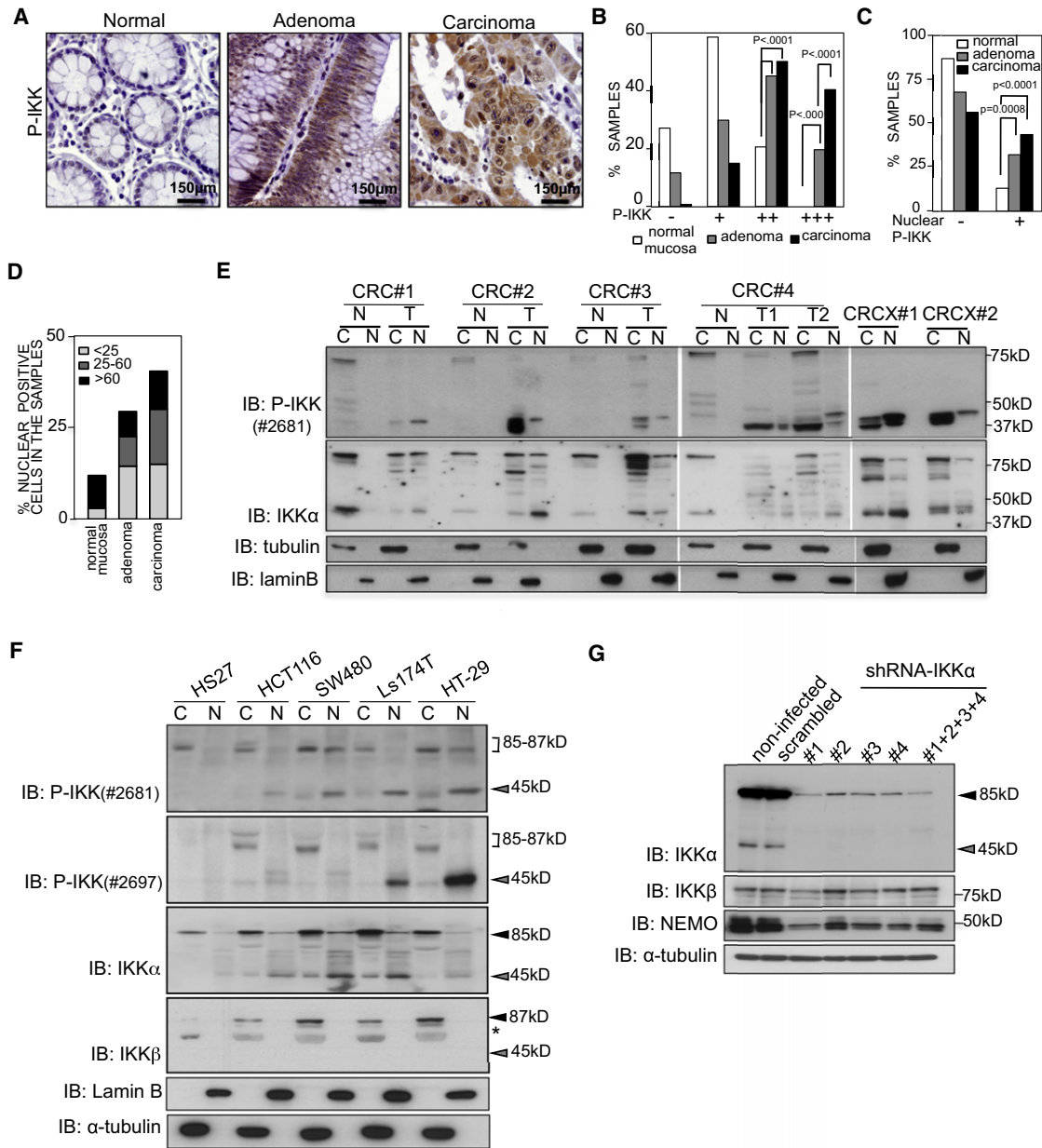
Figure 1. CRC Cells Express a Truncated and Active Form of IKKα in the Nucleus

(A) IHC with α-P-IKKα/βs from normal, adenoma and carcinoma samples (400×) from a human colon tissue microarray including 288 tumor samples.

(B) Normal mucosa, adenoma, and CRC samples were classified based on intensity of α-P-IKKα/β staining.

(C) Samples were classified depending on the presence or absence of nuclear α-P-IKKα/β staining.

(D) Percentage of positive nuclei in samples with P-IKK staining.

(E) Western blot analysis of cytoplasmic and nuclear extracts from human CRC samples and their normal adjacent tissue and two human CRC samples grown as xenografts in nude mice.

(F) Western blot analysis of cytoplasmic and nuclear extracts from different CRC cell lines (HCT116, SW480, Ls174T, HT-29) and nontransformed cell line HS27.

(G) Western blot analysis of total cell extracts from HCT116 cells transduced with shRNA against IKKα or with a scrambled shRNA. IKKβ levels are shown to test isoform specificity.

In (B) and (C), Fisher's exact test was used to determine p values. In (E)–(G), tubulin and lamin B were used as fractionation and loading controls. C, cytoplasmic; N, nuclear. See also Figure S1.

cell carcinomas (Liu et al., 2006). First, we performed single-strand conformational polymorphism (SSCP) analysis of this region, amplified using intronic primers from genomic DNA corresponding to 161 human CRC samples (5 stage I, 52 stage II, 83 stage III, and 21 stage IV). In this screening, we did not detect any alteration beyond a single nucleotide change in an

intronic region of sample 515T (Figure S2A; data not shown). By direct sequencing, we confirmed the absence of mutation in this region using genomic DNA from HCT116, HT-29, and SW480 cells, as well as 16 human CRC samples. Interestingly, analysis of the cDNA identified a deletion of exon 14 in one of the samples that led to a frameshift that generates a premature STOP codon at position 520 (data not shown). Together, these data indicate that mutation of the IKKα gene is not the main mechanism contributing to p45-IKKα generation.

Next, we investigated whether p45-IKKα was produced by FL-IKKα processing. With this objective, we transduced HEK293T, HCT116, and HT-29 cells with a retroviral vector codifying for FL-IKKα fused to the myc epitope at the N-terminal end (myc-IKKα). Western blot analysis of the lysates demonstrated the presence of the expected 85 kDa IKKα protein, in addition to a 45 kDa that was recognized with the α-myc antibody (Figure 2A). In HEK293T cells, myc-IKKα generated a pattern of bands that was identical to the endogenous IKKα from CRC cells (Figure S2B), although p45 was more prominent in CRC cells. Identity of the 45 kDa band was further established by precipitation of HA-IKKα with the α-HA antibody followed by detection with specific α-IKKα antibody generated against its N-terminal end (Figure 2B) and by conventional mass spectrometry analysis of the tryptic peptides (data not shown). Generation of p45-IKKα from HA-IKKα was not modified by mutation of serines 176 and 180 to alanine (S176/180A) or glutamic acid (S176/180E), indicating its activation status was not necessarily linked with cleavage (Figure S2C). These results indicate that FL-IKKα generates p45-IKKα, which comprises the N-terminal kinase and the ubiquitin-like domain (ULD) but lacks the regulatory scafold/dimerization domain (SDD) (Figure 2C). Since IKK exhibits a conformation that involves the physical interaction of SDD with the ULD and kinase domains (Xu et al., 2011), we predicted that p45-IKKα might differentially expose the regions close to the cleavage site compared with FL-IKKα. Based on this, and to further study the distribution and prevalence of p45-IKKα in human samples, we generated monoclonal antibodies against peptide amino acids (aa) 241–424 of human IKKα and tested for their capacity to precipitate p45-IKKα from nondenatured CRC cell lysates. Among these antibodies, we obtained the clone 881H3 that preferentially binds p45-IKKα from tumor cell lysates compared with the full-length (FL) nondenatured form (Figure S2D) and generated a specific staining pattern in WT MEF that was not detected in IKKα KO cells (Figure S2E). In CRC cells, staining with the 881H3 antibody was found in the nucleus and cytoplasm and was lost in cells treated with shRNA against IKKα (Figure S2F). Thus, we selected 881H3 to study the distribution of p45-IKKα by IHC in human samples. In CRC samples, 881H3 generated a specific staining pattern that resembled active P-IKKα including cytoplasmic vesicles and discrete nuclear dots (Figures 2D and 2E). By double IHC and confocal microscopy analysis, we detected a substantial colocalization of p45-IKKα with P-IKK in CRC (Figure 2F). As a control, staining with 881H3 in CRC was lost after incubation with the blocking peptide (Figure S2G). Positive staining for p45-IKKα was also detected in normal colonic mucosas previously categorized as negative for P-IKK, mainly restricted to the proliferative basal regions (Figure S2H). By crossing our

data from active IKK (P-IKK) and p45-IKKα expression, we found that detection of p45-IKKα levels was independent of P-IKK status in the normal mucosa but it was associated in the CRC group of samples (Figures 2D and 2G). A more detailed study of the correlation between p45-IKKα and P-IKK staining demonstrated that p45-IKKα levels significantly and positively correlated with P-IKK reactivity in CRC samples (Figure 2H).

Cathepsin-Mediated Processing Generates p45-IKKα In Vitro

To identify putative proteases that mediate IKKα processing, we created a Python script and queried for candidates using the information in the MEROPS peptidase database (Rawlings et al., 2010). This search was performed using the region including exons 13–14 as a target sequence (aa 300–450). We identified three putative cleavage sites for caspase 3/6/7, cathepsin B/L and cathepsin K that could account for the generation of p45-IKKα (Figure 3A). To test whether these sites were functional, we designed an expression vector containing the myc tag fused to the aa 300–450 IKKα fragment that includes all three sites. We found that this IKKα fragment expressed in HEK293T cells generated a 25 kDa band when incubated at acid pH (optimal for cathepsin activity), which was further increased after incubation with nuclear extracts from Ls174T CRC cells (Figure 3B). Treatment with z-FA-FMK, a specific inhibitor of cathepsin B and L (Sillence and Allan, 1997) but not with the caspase inhibitor z-VAD (not shown), significantly reduced IKKα processing in these experiments (Figure 3C). Next, we generated point mutants of the FL-IKKα construct to disrupt each of the identified protease recognition sites individually and in combination. As shown in Figure 2A, we found that myc-IKKα expressed in HCT116 cells was efficiently processed into p45-IKKα; however, single mutations in cathepsin or caspase sites, and the triple mutation of all three protease recognition sites (3M) reduced IKKα cleavage (from 45% in the WT to 9%–10%, 12%, and 6% in the mutants, respectively). Similarly, the IKKα-3M mutant failed to be processed in nontransformed cells (Figure 3D). These results suggest that all three sites might contribute to some extent to p45-IKKα generation. To further define the cleavage site for p45-IKKα generation, we performed a more detailed analysis of the mass spectrometry data obtained from the precipitated HA-p45-IKKα fragment. In these experiments we failed to detect most of the central region of the IKKα protein (were cleavage is predicted to occur) but we identified a single peak (extracted ion chromatogram) compatible with the expected end-terminal sequence generated from Cathepsin B/L cleaved IKKα protein after trypsin digestion (peptide TVYEGPFAS). In contrast, we did not detect any tryptic peptide with the characteristics of a Caspase- or Cathepsin K-processed IKKα fragment (not shown). Together, these results indicate that p45-IKKα is generated by specific protease activity, most likely through cathepsins.

p45-IKKα Is Generated by Cathepsin-Dependent Processing In Vivo

To investigate the putative involvement of cathepsins in generating p45-IKKα in vivo, we ectopically expressed FL-IKKα alone
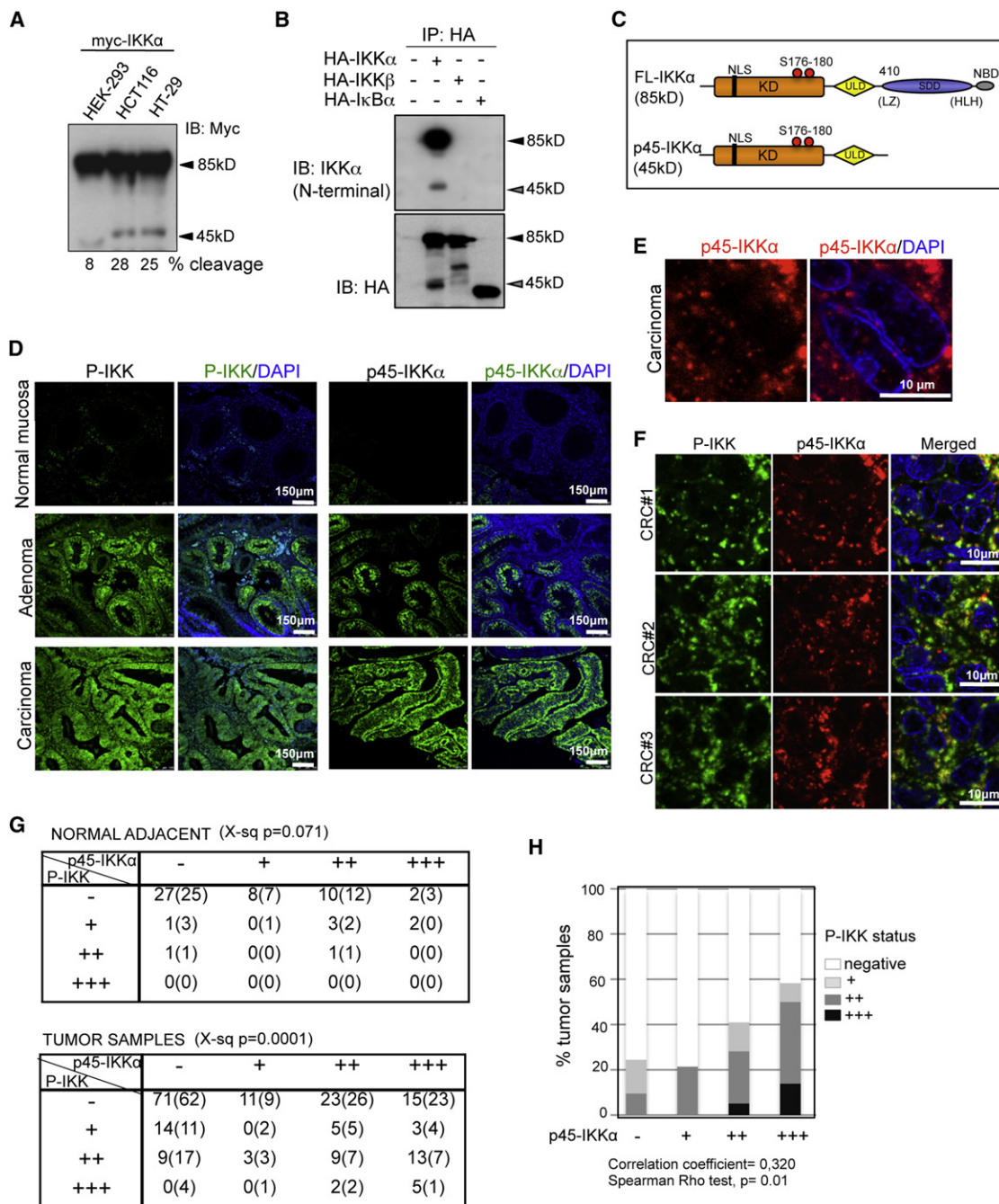
Figure 2. p45-IKKα Is Generated by Proteolytic Processing of the Full-Length Form and Corresponds to the Amino-Terminal Half of the Kinase

(A) Cell lines were transduced with a retroviral vector expressing myc-IKKα. Total lysates were analyzed by western blot using an antibody against the myc epitope (9E10 clone).

(B) HEK293T cells were transfected with HA-IKKα, HA-IKKβ, and HA-IκBα, and, 48 hr after transfection, cell lysates were immunoprecipitated with α-HA antibody and the precipitates were analyzed by western blot with α-HA and α-IKKα antibodies. One of three independent experiments performed is shown.

(C) Schematic representation of FL-IKKα that contains the kinase domain, the ubiquitin-like domain (ULD), an elongated α-helical scaffold/dimerization domain (SDD), including the regions previously characterized as LZ and HLH domains, and the NEMO-binding domain (NBD). Predicted truncated p45-IKKα includes the kinase domain but lacks the SDD and the NBD regions.

(D) Serial sections of human intestinal mucosa, adenoma, and carcinoma samples were stained with α-P-IKK and anti-p45-IKKα (881H3) antibodies and visualized by confocal microscopy.

(E) Detail of nuclear and cytoplasmic p45-IKKα staining in one CRC sample.

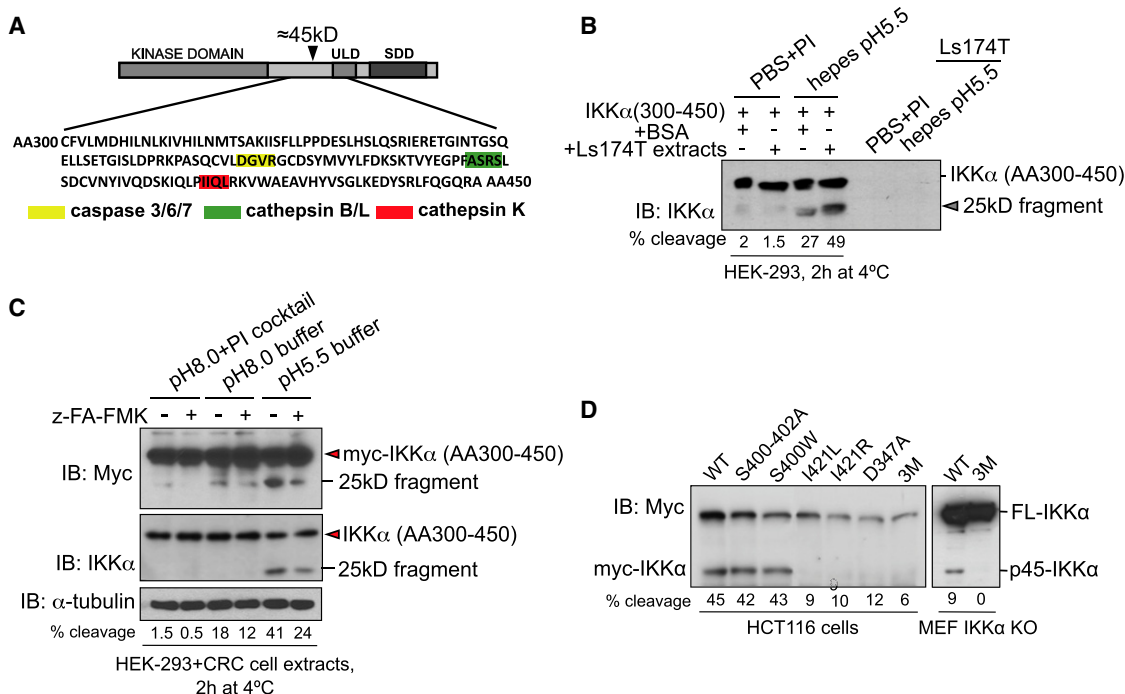(F) Colocalization of p45-IKKα with P-IKK staining in three different CRCs.

Figure 3. p45-IKKα Is Generated In Vitro by Cathepsin-Mediated Processing

(A) Bioinformatic analysis of the region including AA 300–450 of IKKα revealed the presence of putative protease cleavage sites for caspase 3/6/7, cathepsin B/L, and cathepsin K.

(B) HEK293T cells expressing the MT-IKKα 300–450 construct were lysed in PBS plus protease inhibitor cocktail (pH 8.0) or 10 mM HEPES (pH 5.5). Cell lysates were incubated with two volumes of 100 mg/ml BSA or Ls174T lysates for 2 hr at 4°C and western blot analysis was performed.

(C) HEK293T cells expressing MT-IKKα 300–450 WT were lysed in pH 8.0 plus protease inhibitor cocktail buffer, pH 8.0 buffer or pH 5.5 buffer with or without 20 mM z-FA-FMK as indicated, in the presence of LS174T lysates, incubated for 2 hr at 4°C and analyzed by western blot.

(D) HCT116 cells (left) or IKKα KO MEFs (right) expressing myc-IKKα WT or the indicated mutants were lysed in buffer containing protease inhibitors and analyzed by western blot. All the experiments were repeated a minimum of three times with comparable results. Percentage of cleaved IKKα relative to the FL or the aa 300–450 fragment (determined by densitometry from a representative experiment) is shown at the bottom of each lane.

or together with cathepsin B, L, K or caspase 3 in HEK293T cells. We found that expression of either cathepsin homolog increased generation of p45-IKKα compared with cells transfected with control vector (Figure 4A) or caspase 3 (Figure S3A). In agreement with the possibility that cathepsins mediate IKKα cleavage in CRC cells, we found increased levels of cathepsin L (Figure 4B) and B (data not shown) in both nuclear and cytoplasmic lysates, associated with high cathepsin B/L activity (Figure 4C) in all tested CRC cell lines compared with nontransformed HS27 cells. However, cathepsin B/L activity does not strictly correlate with levels of active p45-IKKα in each individual cell line, indicating that cathepsin-mediated processing is a tightly regulated process. Most important, abrogation of cathepsin B/L activity by the pharmacological inhibitor z-FA-FMK mostly abolished formation of endogenous nuclear p45-IKKα in CRC cells (Figures 4D and S3B). By IF followed by confocal microscopy analysis, we detected high levels of cathepsin B and L in human primary

CRC tumors that colocalized with P-IKK in specific ring-shaped cytoplasmic vesicles reminiscent of lysosomal or endosomal structures (Figures 4E and S3C). In these vesicles, P-IKK appeared restricted to the membrane rings where it costains with the specific α-IKKα antibody (Figure S3D), when compared with the more central localization of cathepsins B or L. Different controls for cross-reaction of antibodies or cross-contamination of fluorochromes were performed (Figure S3E). Further characterization of these structures demonstrated that they contained RAB5, a small GTPase protein involved in trafficking of early endosomes (Poteryaev et al., 2010) (Figure 4F), and we found colocalization between P-IKK and some vesicles positive for the late endosomal marker RAB7 (Figure 4G). In contrast, P-IKK detection absolutely diverged from staining with the autophagosomal marker LC3 (Figure S3F) and the lysosomal marker LAMP1 (Figure S3G), excluding the possibility that in cancer cells active p45-IKKα is part of a degradation product.

(G) A group of 183 human colon tumors and 55 normal mucosas, previously characterized for P-IKK, were analyzed by IHC for the presence of p45-IKKα. Tables represent the distribution of p45-IKKα staining in samples categorized as negative or positive (+, ++, and +++) for P-IKK. Statistical analysis demonstrated that P-IKK and p45-IKK expression was distributed randomly in the normal mucosa (X-square test, p = 0.07) but strongly associated in the CRC samples (p = 0.0001).

(H) Spearman Rho test demonstrated a linear positive correlation between P-IKK and p45-IKK levels, which reached statistical significance (p = 0.01).
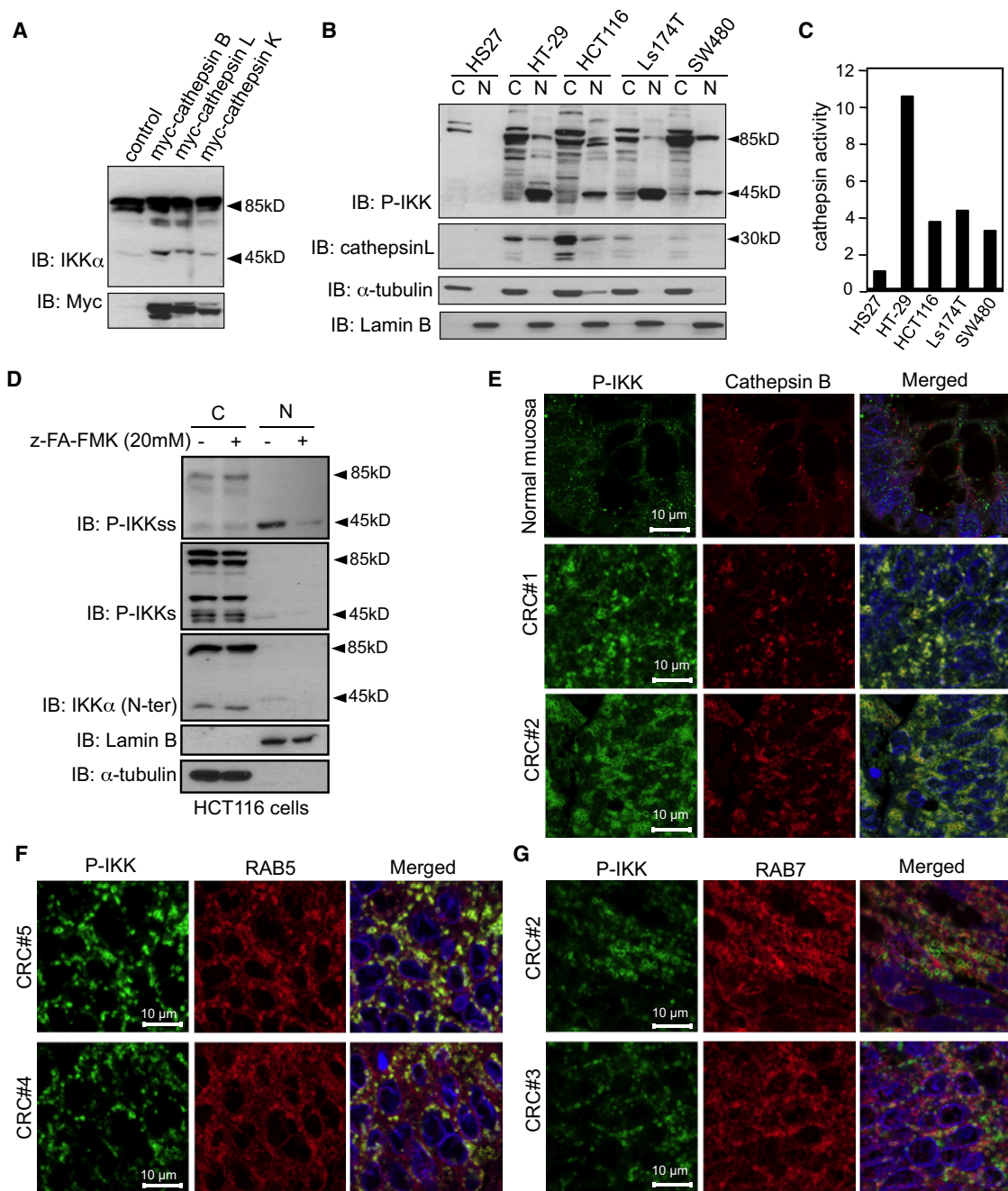See also Figure S2.

Figure 4. Cathepsin-B and L Promote the Formation of p45-IKKα In Vivo

(A) HEK293T cells expressing MT-IKKα were cotransfected with control vector, MT-cathepsin B, MT-cathepsin L, or MT-cathepsin K. Forty-eight hours after transfection, cell lysates were obtained and analyzed by western blot to determine the levels of p45-IKKα.

(B) Western blot analysis of nuclear and cytoplasmic extracts to determine Cathepsin L levels from the indicated cell lines.

(C) Cathepsin activity from the indicated CRC cell lines was determined compared with the nontransformed HS27 cells.

(D) HCT116 cell cultures were incubated for 16 hr with or without z-FA-FMK (20 mM). Cytoplasmic and nuclear cell extracts were obtained and analyzed by western blot. In (B) and (D), α-Lamin B and α-tubulin were used as fractionation and loading controls.

(E) Confocal images of double staining for P-IKK and cathepsin B in CRC samples.

(F and G) Confocal images of double staining for P-IKK and the endosomal markers RAB5 (F) and RAB7 (G). Representative images were selected to illustrate the degree of colocalization between different proteins in CRC.

Scale bars, 10 μm. All experiments were performed in triplicates with comparable results. See also Figure S3.

Of note, in these samples cathepsin B was only partially distributed in the lysosomal particles (Figure S3H).

Together, these results indicate that cathepsin activity is mainly responsible for generating p45-IKKα in CRC cells and suggest that the interaction between IKKα and cathepsins takes place in specific endosomal vesicles. Sorting of IKKα into these vesicles might contribute to regulate IKKα processing.

Truncated IKKα Displays Specific Biochemical Properties

To study the biochemical characteristics of p45-IKKα, we performed gel filtration experiments in Superdex S200 columns from HCT116 (Figure 5A) and SW480 nuclear extracts (Figure S4A) and determined the distribution of active IKKα in the different fractions. We found that active/phosphorylated p45-IKKα coeluted with the nonactive FL-IKKα and NEMO in the high molecular weight (HMW) fractions (19–25) (larger than 210 kDa), whereas FL-active P-IKKα was recovered in low molecular weight (LMW) fractions 38–45, likely corresponding to monomeric IKKα (Figures 5A and S4A). Further suggesting that p45-IKKα was in a HMW complex with nonactive FL-IKKα and NEMO, p45-IKKα expressed in IKKα KO MEFs eluted in intermediate molecular weight fractions 26–36 (Figure 5B, left panels) and partially shifted to HMW fractions 19–24 when FL-IKKα was reintroduced, coeluting with exogenous IKKα and NEMO (Figure 5B, right panels). Existence of this complex was confirmed by precipitation of endogenous NEMO from fractionated nuclear HCT116 extracts (fractions 20–25) (Figure 5C) and total cell lysates (Figure S4B) and detection of both p45 and FL-IKKα in the precipitates. Different amounts of NEMO, FL-IKKα, and p45-IKKα in the precipitates from the fractions suggest the existence of specific complexes with diverse stoichiometries. To study whether IKKβ participates in this complex, we precipitated myc-p45-IKKα expressed in HEK293T cells together with HA-IKKα or HA-IKKβ. We found that HA-IKKα but not HA-IKKβ associated with p45-IKKα in these conditions (Figure 5D).

Nuclear IKKα has been shown to be associated with the chromatin through histone H3 (Zhu et al., 2007a). By pull-down assays, we found that FL-IKKα but not p45-IKKα alone associates with histone H3 (Figure 5E); however, p45-IKKα can bind histone H3 in the presence of FL-IKKα (Figure 5E). In agreement with these results, we found that IKKα associates with histone H3 through its C-terminal region (Figure S4C). Importantly, ectopically expressed p45-IKKα localized essentially in the cytoplasm (although it retains the NLS sequence, see Figure 2C) in the absence of endogenous IKKα, and was redistributed into the nuclear and chromatin compartments in the presence of ectopic FL-IKKα, as shown by western blot from IKKα-deficient MEFs (Figure 5F). However, treatment of these cells with the nuclear export inhibitor Leptomycin B resulted in the accumulation of both FL-IKKα and p45-IKKα in the nucleus (Figure S4D), indicating that NLS is functional in p45-IKKα but its chromatin binding and nuclear retention require the participation of FL-IKKα.

p45-IKKα Promotes Phosphorylation of Specific Substrates Both In Vitro and Vivo

We have previously shown that SMRT and N-CoR corepressors are substrates for IKKα kinase in CRC cells (Fernández-Majada

et al., 2007a, 2007b). To identify the nuclear fraction that contains this kinase activity, we performed immunoprecipitations of Superdex S200 fractions 19–25 (HMW) and 38–45 (LMW) from HCT116 nuclear extracts with either α-IKKα or α-P-IKK antibodies and assayed the capacity of the precipitates to phosphorylate glutathione S-transferase (GST)-N-CoR or GST-SMRT fusion proteins. Precipitates obtained from the HMW fractions (19–25) containing active p45-IKKα, but not precipitates from fractions 38–45 (LMW) including active FL-IKKα (Figure 6A), phosphorylated both N-CoR (Figure 6B) and SMRT (Figure S5A) in vitro.

To further test whether p45-IKKα was involved in phosphorylating nuclear substrates in vivo, we transfected HA-FL-IKKα, truncated active MT-p45-IKKα or both constructs in IKKα KO MEFs and measured their effect on different substrates by western blot analysis. In agreement with the in vitro data, active p45-IKKα induced SMRT phosphorylation in serine 2410 and this effect was enhanced by FL-IKKα. In addition, combination of active p45-IKKα and FL-IKKα induced phosphorylation of histone H3 (Figure 6C). These results indicate that p45-IKKα is required for specific nuclear IKKα kinase activities, although p45-IKKα by itself was unable to associate (Figure S5B) or phosphorylate SMRT or NCoR in vitro (not shown). We also measured the transcriptional effects of reintroducing FL- or p45-IKKα in IKKα KO cells. As shown in Figure 6D, ectopic expression of FL-IKKα induced the activation of several genes known to be repressed by SMRT such as *hes1*, *herp2*, and *hes5*. This effect was potentiated by p45-IKKα coexpression whereas p45-IKKα alone did not have any transcriptional effect.

Next, we investigated whether phosphorylation of nuclear IKKα targets and transcription of SMRT-repressed genes in CRC cells depends on p45-IKKα. To do this, we transduced HCT116 or HT-29 cells with retroviral vectors containing an IRES-GFP and codifying for WT IKKα, the IKKα 3M mutant alone or 3M together with p45-IKKα. Next, we sorted the GFP positive cells and knocked down endogenous IKKα using shRNA that targets its 3′ untranslated region (UTR) (shRNAno. 4, Figures 1G and S1C), which does not affect the IKK constructs. Efficiency of endogenous IKKα depletion and expression of the different IKKα constructs was confirmed by western blot of sorted cells (Figure 6E). We found that WT IKKα, but not the IKKα-3M mutant, restored or even increased phosphorylation of SMRT and histone H3 in IKKα knocked down CRC cells. Similar effects were observed when p45-IKKα was coexpressed with noncleavable IKKα (Figure 6E). In contrast, IKKα-3M efficiently binds to IKKβ (Figure S5C), induces IκBα phosphorylation (Figure 6F) and was activated by the IKK kinase TAK1 (Figure 6G). Most importantly, changes in SMRT phosphorylation induced by IKKα reconstitution correlated with changes in the transcriptional activity of specific SMRT targets, including the antiapoptotic gene *cIAP2* (Figure 6H).

Truncated P-IKKα Is Required for Preventing Apoptosis and Supporting the Growth of CRC Cells

Finally, we measured the contribution of IKKα and p45-IKKα activities to CRC. Indicative of their functional relevance,
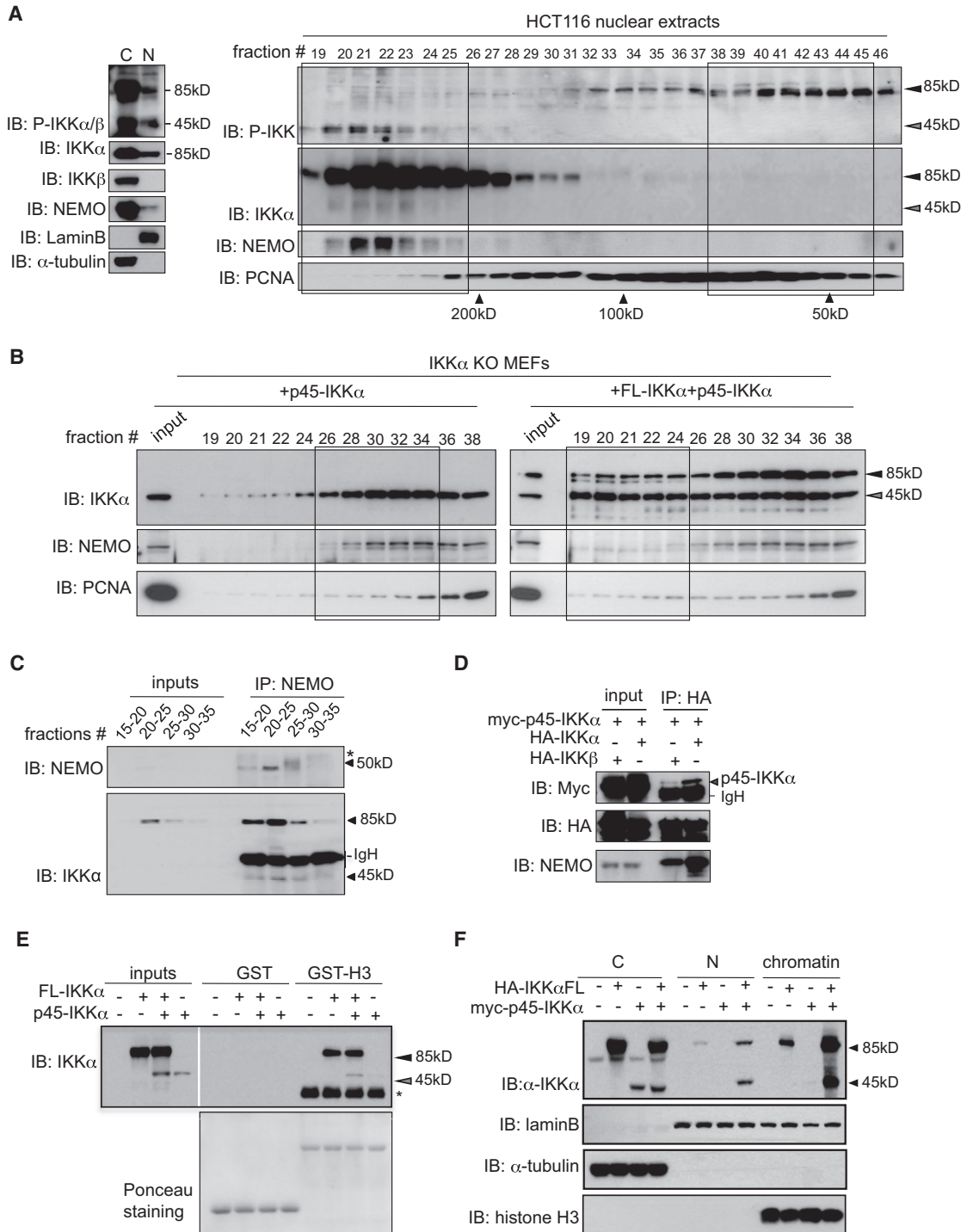
Figure 5. P45-IKKα Associates with Nuclear NEMO in CRC Cells

(A) Western blot analysis of cytoplasmic and nuclear extracts from HCT116 cells using the indicated antibodies (left). HCT116 nuclear extracts (100 μl) were loaded on a Superdex200 column. One drop (40 μl approximately) per fraction was collected and analyzed by western blot with the indicated antibodies (right).

(B) IKKα KO mouse embryonic fibroblasts (MEFs) were transfected with p45-IKKα (left panels) or p45-IKKα plus FL-IKKα (right panels). Seventy-two hours after puromycin selection, whole-cell extracts were obtained and lysates were loaded on a Superdex200 column. One drop per fraction was collected and analyzed by western blot with the indicated antibodies.

(C) HCT116 nuclear extracts were fractionated in Superdex200 column and the indicated fractions were precipitated with the α-NEMO antibody. Western blot analysis demonstrated the presence of endogenous FL-KKα (85 kDa) and p45-IKKα in the precipitates. The asterisk denoted a nonspecific band in the western blot for NEMO.

knocking down IKKα significantly inhibits the growing capacity of all tested CRC cell lines (Figure 7A). Using the same strategy as before (transducing WT IKKα or the 3M mutant or the IKKα mutant plus p45-IKKα, followed by endogenous IKKα knockdown), we tested whether p45-IKKα was required to revert IKKα depletion in CRC cells. We found that the effects of IKKα knockdown in CRC cell growth were specifically rescued by WT IKKα or by the IKKα 3M mutant plus p45-IKKα but not by IKKα 3M alone (Figure 7B). Flow cytometry analysis demonstrated that only IKKα or 3M plus p45-IKKα protected CRC cells from apoptosis, as measured by annexin V binding (Figure 7C) and induced a slight, but significant, increase in cell proliferation (Figure 7D). Prosurvival effects of p45-IKKα can be explained, at least in part, by regulation of CIAP2 (Deveraux et al., 1998). We next determined the capacity of HCT116 and HT-29 cells depleted from endogenous IKKα and reconstituted with WT or the noncleavable IKKα mutant to grow as tumor xenografts in nude mice. CRC cells expressing WT IKKα generated significantly larger tumors than cells expressing the IKKα mutant (Figures 7E–7G and S6), indicating the pathological relevance of p45-IKKα.

In summary, we have identified a cathepsin-dependent mechanism that generates truncated IKKα, which is found in the nucleus of tumor cells in its active form, where it is responsible for specific kinase activities that directly impinge on cancer cell growth both in vitro and in vivo.

DISCUSSION

Our results indicate that human CRC tumors display constitutive nuclear IKKα phosphorylation, associated with increased tumor grade. In tumor cells, we found that IKKα is proteolytically processed into a 45 kDa fragment, in a cathepsin-dependent manner. Moreover, p45-IKKα and P-IKK levels showed a significant correlation in CRC samples. At the functional level, we found that nuclear active p45-IKKα coelutes and interacts with nonphosphorylated FL-IKKα and NEMO and is capable of phosphorylating SMRT and N-CoR corepressors and histone H3. Cleavage of IKKα into p45-IKKα is required for tumor growth in vitro and in vivo, although we detected some p45-IKKα and P-IKK staining in few normal samples mainly restricted to the proliferative compartment. The physiological significance of p45-IKKα and the mechanisms regulating its generation, activation, and nuclear translocation are currently being investigated.

Although IKKα is mostly found in the cytoplasm associated with IKKβ and NEMO, we here demonstrate that truncated p45-IKKα translocates to the nuclear compartment in CRC cells where it interacts with FL-IKKα and NEMO. Which are the mechanisms regulating formation of this IKK complex remain unknown, but they might include availability of IKK components (i.e., low amounts of nuclear IKKβ compared with nuclear IKKα and intermediate levels of NEMO), posttranslational modifications of specific elements and the participation of adaptor proteins.

On the other hand, it is known that IKKα phosphorylates specific nuclear targets such as histone H3 and nuclear corepressors (Anest et al., 2003; Hoberg et al., 2004; Yamamoto et al., 2003). Here, we show that p45-IKKα is required for SMRT and histone H3 phosphorylation. By analysis of the elution fractions from Superdex S200 columns, we detected that all the FL-P-IKKα eluted in a LMW fraction compatible with monomeric IKK, which is unable to phosphorylate SMRT. Which are the substrates of nuclear FL-P-IKK kinase remains to be elucidated. On the other hand, FL-IKKα is required for chromatin binding of p45-IKKα association with SMRT and phosphorylation of SMRT and histone H3 by p45-IKKα, although it retains the kinase domain and NLS sequences. In this sense, it has been recently demonstrated the importance of the SDD domain of IKKβ (that is conserved in IKKα) not only for substrate recognition but also for kinase activation (Xu et al., 2011). We propose that p45-IKKα uses the SDD and NBD domains from FL-IKKα to achieve their functions.

Mechanisms that lead to the formation of p45-IKKα may not be unique and are likely context dependent. Examples include frameshift mutations generating premature STOP codons that are present in squamous cell carcinoma (Liu et al., 2006) and splicing variants that codify for proteins lacking the SDD as it was found in T-lymphocytes and in the brain (McKenzie et al., 2000). However, we did not find such mutations in around 200 samples analyzed, and identified alternative splicing of exon 14 (leading to truncated IKKα) in only one CRC sample. Thus, we propose that the main source of p45-IKKα in CRC cells is proteolytic processing of IKKα by cathepsins. This is consistent with increased cathepsin activity found in CRC that can be associated with the enhanced aerobic glycolysis, previously described by Warburg (Swietach et al., 2007), but also with other cancer-related pathways such as erbB2-K-RAS (Fehrenbacher et al., 2008; Kim et al., 1998), JAK-STAT (Kreuzaler et al., 2011), or vitamin D-cystatin (Alvarez-Díaz et al., 2009). In addition, we found that mutations in a caspase consensus site of IKKα also reduced p45-IKKα generation, which might suggest that the presence of adjacent protease binding sites might facilitate cathepsin recognition or that the caspase site is functional under specific conditions. Whether cathepsin-mediated processing is differentially required to generate cytoplasmic or nuclear p45-IKKα is somewhat puzzling and requires further investigation. Most important, in CRC cells cathepsin B and L colocalized

(D) HEK293T cells were transfected with HA-IKKα or HA-IKKβ and MT-p45-IKKα. Forty-eight hours after transfection cell lysates were immunoprecipitated with α-HA. Western blot analysis showed that MT-p45-IKKα precipitates with HA-IKKα but not with HA-IKKβ.

(E) Pull-down assay with GST-H3 and cell lysates from HEK293T cells transfected with HA-FL-IKKα, HA-FL-IKKα plus MT-p45-IKKα, or MT-p45-IKKα alone. The presence of IKKα or p45-IKKα in the precipitates was determined by western blot. Ponceau staining of GST proteins is shown. Inputs represent 10% of the lysate. The asterisk indicates a nonspecific band corresponding to GST-H3 that was detected with α-IKKα antibody.

(F) IKKα-deficient MEFs were transfected with control vector, HA-IKKα, MT-p45-IKKα, or both constructs. Cytoplasmic, nuclear and chromatin fractions were obtained and analyzed by western blot with α-IKKα antibody. Levels of tubulin, laminB, and histone H3 are shown as fractionation and loading controls.

All experiments were repeated at least three times with comparable results. See also Figure S4.
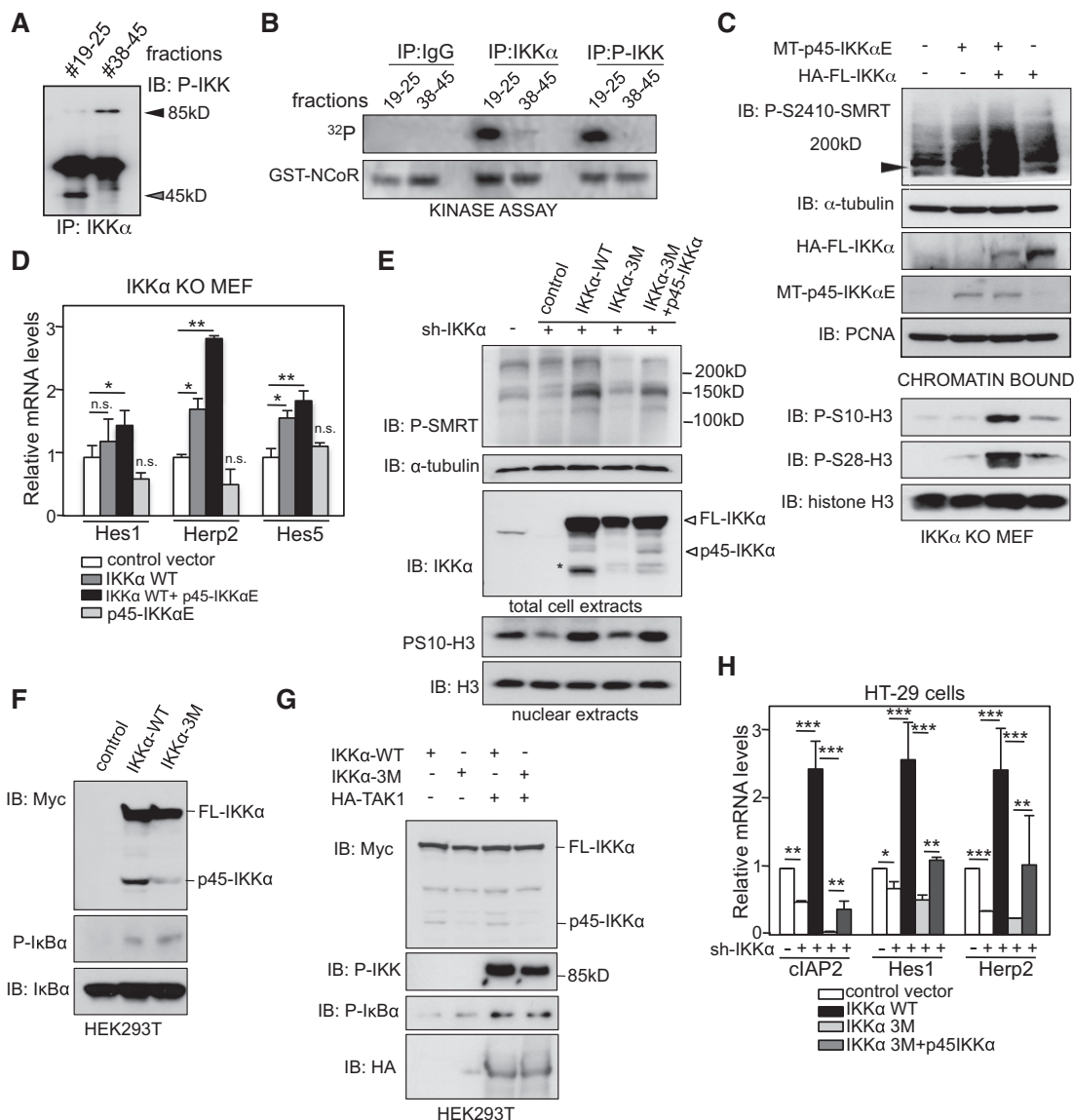
Figure 6. p45-IKKα Promotes Phosphorylation of Specific Substrates Both In Vitro and Vivo

(A) α-IKKα precipitates from fractions 19–25 and 38–45 and western blot analysis to determine the presence of FL or truncated active IKKα.

(B) Kinase activity of the α-IKKα and α-P-IKKα/β precipitates from Superdex200 fractions was assayed on GST-NCoR (amino acids 2256–2452) and detected by $_{32}$P incorporation. Total levels of GST-N-CoR protein are shown.

(C) IKKα KO MEFs were transfected with the indicated plasmids and selected for 72 hr with puromycin. Whole-cell extracts or chromatin extracts were obtained and analyzed by western blot with the indicated antibodies. P-SMRT antibody detected different isoforms ranging from 150 to 300 kDa. Levels of α-tubulin, PCNA and histone H3 are shown as loading controls.

(D) Quantitative real-time PCR showing the expression levels of different SMRT-repressed genes in the IKKα KO MEFs reconstituted as described.

(E) Phosphorylation of SMRT and histone H3 was analyzed by western blot analysis in IKKα-depleted HCT116 cells transduced with the indicated IKKα constructs. In the α-IKKα blot, the asterisk indicates the p45 fragment generated from FL-IKKα and arrows indicate the unprocessed proteins codified by exogenous FL-IKKα and p45-IKKα constructs.

(F) Western blot showing the levels of IκBα phosphorylation in cells transduced with the indicated constructs.

(G) Western blot showing phosphorylation of exogenous myc-IKKα (WT and 3M) and IκBα induced by TAK1.

(H) Expression levels of different SMRT-repressed genes in the indicated cell pools as determined by quantitative real-time PCR.

In (D) and (H), statistically significance was determined using t test (*p < 0.05; **p < 0.01, ***p < 0.001). Error bars represent SD. All experiments were performed a minimum of three times with comparable results. See also Figure S5.
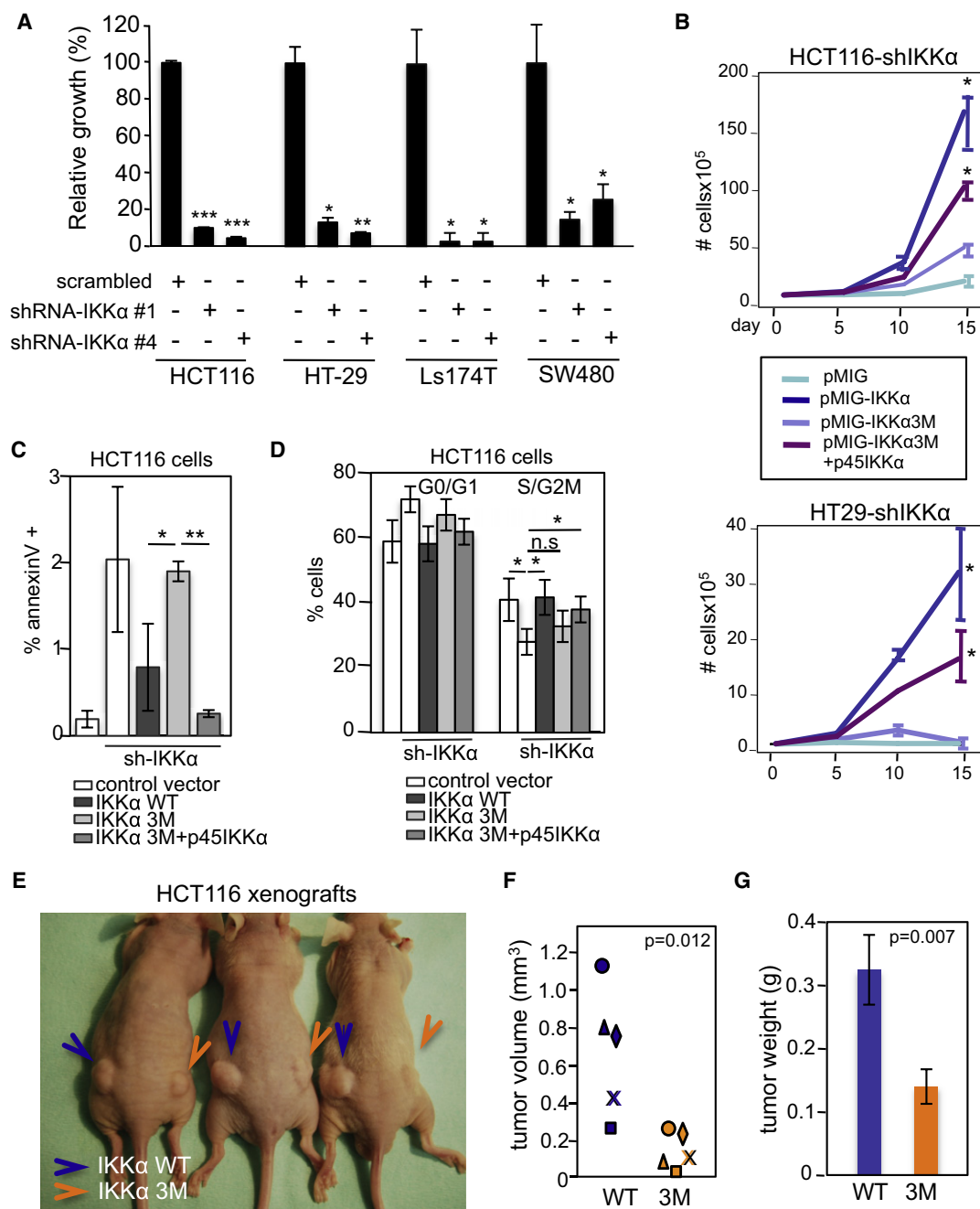
Figure 7. Generation of p45-IKKα Is Required to Maintain CRC Cell Growth In Vitro and in Vivo

(A) Cells transduced with the indicated shRNAs were seeded at 10^3 cells per well (in six-well plates) and quantified after 1 week.

(B) Effects of IKKα depletion and reintroduction of the different IKKα constructs in the proliferation ratio of HCT116 and HT-29 cells.

(C and D) Flow cytometry analysis of AnnexinV binding (C) and cell cycle (D) in HCT116 cells transduced with the indicated constructs.

(E) Generation of tumor xenografts from HCT116 cells expressing WT or the noncleavable IKKα 3M mutant. Three representative from five animals included in this experiment are shown.

(F and G) Measurement of tumor size (F) and weight (G) 3 weeks after injection.

Statistical significance was determined using t test (*p < 0.05; **p < 0.01; n.s., no significance). Error bars represent SD. See also Figure S6.

with P-IKK in cytoplasmic ring-shape structures, corresponding to endosomal vesicles that express RAB5, suggesting that IKKα processing and activation occurs previous to its nuclear translo-

cation. Similar mechanisms of endosomal-mediated processing have been shown to regulate ligand-independent activation of Notch (Wilkin et al., 2008), activation of interferon response

through TLR4 (Kagan et al., 2008; Tseng et al., 2010), death signaling induced by the TNF-α receptor (Schneider-Brachert et al., 2004), and dorsoventral specification in *Drosophila* (Lund et al., 2010).

Interestingly, our results indicate that p45-IKKα is not restricted to CRC since nonphosphorylated forms are consistently found in the cytoplasm of nontransformed MEF and human colonic mucosa. However, homozygous mutations of human IKKα leading to a premature STOP codon at position 422 results in a lethal syndrome due to severe fetal malformation defects (Lahtela et al., 2010), indicating the functional requirement of one FL allele. Further work, including generation of new animal models should decipher the physiological and pathological contribution of p45-IKKα. However, we found that cancer cells lacking IKKα cannot form tumors in vivo when reconstituted with a noncleavable IKKα mutant.

The relevance of this work resides in the characterization of p45-IKKα, which function is not directly related with NF-κB but holds important tumorigenic potential. This finding opens the possibility of designing new anticancer treatments targeting IKKα cleavage that should restrict the negative effects of inhibiting general IKK activity and thus NF-κB. In addition, we have generated an antibody that specifically recognizes p45-IKKα by IHC, IF, and IP of CRC samples, which in the near future will be applicable, likely in combination with P-IKK detection, for analysis of human tumors, stratification of CRC patients, and other clinical-related applications.

EXPERIMENTAL PROCEDURES

Human Colorectal Samples
Samples from patients were obtained from the archives of the Tumor Bank of Hospital del Mar. All patients gave written consent to donate the tumor specimen. The ethics committee of our institution approved the study.

Production of Monoclonal Antibodies against p45-IKKα
These antibodies were generated by Abyntek (Spain) using the peptide aa 241–424 of human IKKα as immunogen.

Gel Filtration Assay on Superdex200 Column
HCT116 nuclear extracts (100 μl) were lysed in PBS containing 0.5% Triton X-100, 1 mM EDTA, 100 mM Na-orthovanadate, 0.25 mM phenylmethanesulfonylfluoride (PMSF), and complete protease inhibitor cocktail (Roche, Basel, Switzerland), centrifuged, and loaded on Superdex200 gel filtration column (GE Healthcare). One drop (40 μl) per fraction was collected and analyzed by western blot.

Protein Kinase Assays
Nuclear fractions 19–27 and 36–45 from Superdex200 column were precleared and incubated with α-IKKα or α-P-IKKα/β overnight at 4°C. Precipitates were captured with Protein A-Sepharose, washed and assayed for their kinase activity on GST fusion proteins. Kinase reaction was performed at 30°C in 20 mM Tris (pH 7.5), 5 mM MgCl$_2$, and 1 mM DTT.

Statistical Methods
Categorical data were compared by use of Fisher's exact test. A nonparametric analysis of variance was used for the analysis of the ordinal expression of P-IKK data by applying a rank transformation on the dependent variable. Analysis was performed using SAS version 9.1.3 software (SAS Institute Inc., Cary, NC), and level of significance was established at 0.05 (two-sided).

Tumor Xenografts
HCT116 and HT-29 cells were transduced with different IKKα-retroviral vectors and sorted based on YFP expression. Then, cells were transduced with shRNA vectors, selected for 3 days with puromycin, and tested for the expression of the target proteins. Cells (2×10^4) were suspended in matrigel and injected subcutaneously in nude mice, and, after 3 weeks, visible tumors were measured and photographed. Animals were kept under pathogen-free conditions and all procedures approved by the Animal Care Committee.

SUPPLEMENTAL INFORMATION

Supplemental Information includes Extended Experimental Procedures and six figures and can be found with this article online at http://dx.doi.org/10.1016/j.celrep.2012.08.028.

LICENSING INFORMATION

ACKNOWLEDGMENTS

REFERENCES

Alvarez-Díaz, S., Valle, N., García, J.M., Peña, C., Freije, J.M., Quesada, V., Astudillo, A., Bonilla, F., López-Otín, C., and Muñoz, A. (2009). Cystatin D is a candidate tumor suppressor gene induced by vitamin D in human colon cancer cells. J. Clin. Invest. *119*, 2343–2358.

Anest, V., Hanson, J.L., Cogswell, P.C., Steinbrecher, K.A., Strahl, B.D., and Baldwin, A.S. (2003). A nucleosomal function for IkappaB kinase-alpha in NF-kappaB-dependent gene expression. Nature *423*, 659–663.

Anest, V., Cogswell, P.C., and Baldwin, A.S., Jr. (2004). IkappaB kinase alpha and p65/RelA contribute to optimal epidermal growth factor-induced c-fos gene expression independent of IkappaBalpha degradation. J. Biol. Chem. *279*, 31183–31189.

Chen, L.W., Egan, L., Li, Z.W., Greten, F.R., Kagnoff, M.F., and Karin, M. (2003). The two faces of IKK and NF-kappaB inhibition: prevention of systemic inflammation but increased local injury following intestinal ischemia-reperfusion. Nat. Med. *9*, 575–581.

Deveraux, Q.L., Roy, N., Stennicke, H.R., Van Arsdale, T., Zhou, Q., Srinivasula, S.M., Alnemri, E.S., Salvesen, G.S., and Reed, J.C. (1998). IAPs block apoptotic events induced by caspase-8 and cytochrome c by direct inhibition of distinct caspases. EMBO J. *17*, 2215–2223.

DiDonato, J.A., Hayakawa, M., Rothwarf, D.M., Zandi, E., and Karin, M. (1997). A cytokine-responsive IkappaB kinase that activates the transcription factor NF-kappaB. Nature *388*, 548–554.

Fehrenbacher, N., Bastholm, L., Kirkegaard-Sørensen, T., Rafn, B., Bøttzauw, T., Nielsen, C., Weber, E., Shirasawa, S., Kallunki, T., and Jäättelä, M. (2008).

Sensitization to the lysosomal cell death pathway by oncogene-induced down-regulation of lysosome-associated membrane proteins 1 and 2. Cancer Res. 68, 6623–6633.

Fernández-Majada, V., Aguilera, C., Villanueva, A., Vilardell, F., Robert-Moreno, A., Aytés, A., Real, F.X., Capella, G., Mayo, M.W., Espinosa, L., and Bigas, A. (2007a). Nuclear IKK activity leads to dysregulated notch-dependent gene expression in colorectal cancer. Proc. Natl. Acad. Sci. USA 104, 276–281.

Fernández-Majada, V., Pujadas, J., Vilardell, F., Capella, G., Mayo, M.W., Bigas, A., and Espinosa, L. (2007b). Aberrant cytoplasmic localization of N-CoR in colorectal tumors. Cell Cycle 6, 1748–1752.

Fre, S., Huyghe, M., Mourikis, P., Robine, S., Louvard, D., and Artavanis-Tsakonas, S. (2005). Notch signals control the fate of immature progenitor cells in the intestine. Nature 435, 964–968.

Greten, F.R., Arkan, M.C., Bollrath, J., Hsu, L.C., Goode, J., Miething, C., Göktuna, S.I., Neuenhahn, M., Fierer, J., Paxian, S., et al. (2007). NF-kappaB is a negative regulator of IL-1beta secretion as revealed by genetic and pharmacological inhibition of IKKbeta. Cell 130, 918–931.

Hao, L., Rizzo, P., Osipo, C., Pannuti, A., Wyatt, D., Cheung, L.W., Sonenshein, G., Osborne, B.A., and Miele, L. (2010). Notch-1 activates estrogen receptor-alpha-dependent transcription via IKKalpha in breast cancer cells. Oncogene 29, 201–213.

Hayden, M.S., and Ghosh, S. (2004). Signaling to NF-kappaB. Genes Dev. 18, 2195–2224.

Hayden, M.S., West, A.P., and Ghosh, S. (2006). NF-kappaB and the immune response. Oncogene 25, 6758–6780.

Hoberg, J.E., Yeung, F., and Mayo, M.W. (2004). SMRT derepression by the IkappaB kinase alpha: a prerequisite to NF-kappaB transcription and survival. Mol. Cell 16, 245–255.

Kagan, J.C., Su, T., Horng, T., Chow, A., Akira, S., and Medzhitov, R. (2008). TRAM couples endocytosis of Toll-like receptor 4 to the induction of interferon-beta. Nat. Immunol. 9, 361–368.

Kim, K., Cai, J., Shuja, S., Kuo, T., and Murnane, M.J. (1998). Presence of activated ras correlates with increased cysteine proteinase activities in human colorectal carcinomas. Int. J. Cancer 79, 324–333.

Kreuzaler, P.A., Staniszewska, A.D., Li, W., Omidvar, N., Kedjouar, B., Turkson, J., Poli, V., Flavell, R.A., Clarkson, R.W., and Watson, C.J. (2011). Stat3 controls lysosomal-mediated cell death in vivo. Nat. Cell Biol. 13, 303–309.

Lahtela, J., Nousiainen, H.O., Stefanovic, V., Tallila, J., Viskari, H., Karikoski, R., Gentile, M., Saloranta, C., Varilo, T., Salonen, R., and Kestilä, M. (2010). Mutant CHUK and severe fetal encasement malformation. N. Engl. J. Med. 363, 1631–1637.

Liu, B., Park, E., Zhu, F., Bustos, T., Liu, J., Shen, J., Fischer, S.M., and Hu, Y. (2006). A critical role for I kappaB kinase alpha in the development of human and mouse squamous cell carcinomas. Proc. Natl. Acad. Sci. USA 103, 17202–17207.

Luedde, T., Beraza, N., Kotsikoris, V., van Loo, G., Nenci, A., De Vos, R., Roskams, T., Trautwein, C., and Pasparakis, M. (2007). Deletion of NEMO/IKKgamma in liver parenchymal cells causes steatohepatitis and hepatocellular carcinoma. Cancer Cell 11, 119–132.

Lund, V.K., DeLotto, Y., and DeLotto, R. (2010). Endocytosis is required for Toll signaling and shaping of the Dorsal/NF-kappaB morphogen gradient during Drosophila embryogenesis. Proc. Natl. Acad. Sci. USA 107, 18028–18033.

Luo, J.L., Tan, W., Ricono, J.M., Korchynskyi, O., Zhang, M., Gonias, S.L., Cheresh, D.A., and Karin, M. (2007). Nuclear cytokine-activated IKKalpha controls prostate cancer metastasis by repressing Maspin. Nature 446, 690–694.

Maeda, S., Kamata, H., Luo, J.L., Leffert, H., and Karin, M. (2005). IKKbeta couples hepatocyte death to cytokine-driven compensatory proliferation that promotes chemical hepatocarcinogenesis. Cell 121, 977–990.

McKenzie, F.R., Connelly, M.A., Balzarano, D., Müller, J.R., Geleziunas, R., and Marcu, K.B. (2000). Functional isoforms of IkappaB kinase alpha (IKKalpha) lacking leucine zipper and helix-loop-helix domains reveal that IKKalpha and IKKbeta have different activation requirements. Mol. Cell. Biol. 20, 2635–2649.

Nenci, A., Becker, C., Wullaert, A., Gareus, R., van Loo, G., Danese, S., Huth, M., Nikolaev, A., Neufert, C., Madison, B., et al. (2007). Epithelial NEMO links innate immunity to chronic intestinal inflammation. Nature 446, 557–561.

Park, K.J., Krishnan, V., O'Malley, B.W., Yamamoto, Y., and Gaynor, R.B. (2005). Formation of an IKKalpha-dependent transcription complex is required for estrogen receptor-mediated gene activation. Mol. Cell 18, 71–82.

Pasparakis, M., Courtois, G., Hafner, M., Schmidt-Supprian, M., Nenci, A., Toksoy, A., Krampert, M., Goebeler, M., Gillitzer, R., Israel, A., et al. (2002). TNF-mediated inflammatory skin disease in mice with epidermis-specific deletion of IKK2. Nature 417, 861–866.

Poteryaev, D., Datta, S., Ackema, K., Zerial, M., and Spang, A. (2010). Identification of the switch in early-to-late endosome transition. Cell 141, 497–508.

Prajapati, S., Tu, Z., Yamamoto, Y., and Gaynor, R.B. (2006). IKKalpha regulates the mitotic phase of the cell cycle by modulating Aurora A phosphorylation. Cell Cycle 5, 2371–2380.

Rawlings, N.D., Barrett, A.J., and Bateman, A. (2010). MEROPS: the peptidase database. Nucleic Acids Res. 38(Database issue), D227–D233.

Schneider-Brachert, W., Tchikov, V., Neumeyer, J., Jakob, M., Winoto-Morbach, S., Held-Feindt, J., Heinrich, M., Merkel, O., Ehrenschwender, M., Adam, D., et al. (2004). Compartmentalization of TNF receptor 1 signaling: internalized TNF receptosomes as death signaling vesicles. Immunity 21, 415–428.

Schulze-Luehrmann, J., and Ghosh, S. (2006). Antigen-receptor signaling to nuclear factor kappa B. Immunity 25, 701–715.

Senftleben, U., Cao, Y., Xiao, G., Greten, F.R., Krähn, G., Bonizzi, G., Chen, Y., Hu, Y., Fong, A., Sun, S.C., and Karin, M. (2001). Activation by IKKalpha of a second, evolutionary conserved, NF-kappa B signaling pathway. Science 293, 1495–1499.

Sillence, D.J., and Allan, D. (1997). Evidence against an early signalling role for ceramide in Fas-mediated apoptosis. Biochem. J. 324, 29–32.

Song, L.L., Peng, Y., Yun, J., Rizzo, P., Chaturvedi, V., Weijzen, S., Kast, W.M., Stone, P.J., Santos, L., Loredo, A., et al. (2008). Notch-1 associates with IKKalpha and regulates IKK activity in cervical cancer cells. Oncogene 27, 5833–5844.

Swietach, P., Vaughan-Jones, R.D., and Harris, A.L. (2007). Regulation of tumor pH and the role of carbonic anhydrase 9. Cancer Metastasis Rev. 26, 299–310.

Tseng, P.H., Matsuzawa, A., Zhang, W., Mino, T., Vignali, D.A., and Karin, M. (2010). Different modes of ubiquitination of the adaptor TRAF3 selectively activate the expression of type I interferons and proinflammatory cytokines. Nat. Immunol. 11, 70–75.

van Es, J.H., van Gijn, M.E., Riccio, O., van den Born, M., Vooijs, M., Begthel, H., Cozijnsen, M., Robine, S., Winton, D.J., Radtke, F., and Clevers, H. (2005). Notch/gamma-secretase inhibition turns proliferative cells in intestinal crypts and adenomas into goblet cells. Nature 435, 959–963.

Vilimas, T., Mascarenhas, J., Palomero, T., Mandal, M., Buonamici, S., Meng, F., Thompson, B., Spaulding, C., Macaroun, S., Alegre, M.L., et al. (2007). Targeting the NF-kappaB signaling pathway in Notch1-induced T-cell leukemia. Nat. Med. 13, 70–77.

Wilkin, M., Tongngok, P., Gensch, N., Clemence, S., Motoki, M., Yamada, K., Hori, K., Taniguchi-Kanai, M., Franklin, E., Matsuno, K., and Baron, M. (2008). Drosophila HOPS and AP-3 complex genes are required for a Deltex-regulated activation of notch in the endosomal trafficking pathway. Dev. Cell 15, 762–772.

Xu, G., Lo, Y.C., Li, Q., Napolitano, G., Wu, X., Jiang, X., Dreano, M., Karin, M., and Wu, H. (2011). Crystal structure of inhibitor of κB kinase β. Nature 472, 325–330.

Yamamoto, Y., Verma, U.N., Prajapati, S., Kwak, Y.T., and Gaynor, R.B. (2003). Histone H3 phosphorylation by IKK-alpha is critical for cytokine-induced gene expression. Nature *423*, 655–659.

Zandi, E., Rothwarf, D.M., Delhase, M., Hayakawa, M., and Karin, M. (1997). The IkappaB kinase complex (IKK) contains two kinase subunits, IKKalpha and IKKbeta, necessary for IkappaB phosphorylation and NF-kappaB activation. Cell *91*, 243–252.

Zhu, F., Xia, X., Liu, B., Shen, J., Hu, Y., Person, M., and Hu, Y. (2007a). IKKalpha shields 14-3-3sigma, a G(2)/M cell cycle checkpoint gene, from hypermethylation, preventing its silencing. Mol. Cell *27*, 214–227.

Zhu, F., Xia, X., Liu, B., Shen, J., Hu, Y., Person, M., and Hu, Y. (2007b). IKKalpha shields 14-3-3sigma, a G(2)/M cell cycle checkpoint gene, from hypermethylation, preventing its silencing. Mol. Cell *27*, 214–227.